Monte Carlo simulation of a many-fermion study*

D. Ceperley and G. V. Chester
Laboratory of Atomic and Solid State Physics, Cornell University, Ithaca, New York 14853

M. H. Kalos
Courant Institute of Mathematical Sciences, New York University, 251 Mercer Street, New York, New York 10012

(Received 15 December 1976)

The Metropolis Monte Carlo method is used to sample the square of an antisymmetric wave function composed of a product of a Jastrow wave function and a number of Slater determinants. We calculate variational energies for ^{3}He and several models of neutron matter. The first-order Wu-Feenberg expansion is shown always to underestimate the energy, sometimes seriously. The phase diagram for ground-state Yukawa matter is determined. There is a class of Yukawa potentials which do not lead to a crystal phase at any density.

I. INTRODUCTION

In recent years, there have been many Monte Carlo simulations of Bose systems. The simplest of these uses the Metropolis method from classical statistical mechanics to sample a variational Jastrow wave function and to find an upper bound to the ground-state energy.[1,2] Recently, a more complex Monte Carlo algorithm has been used to find exact ground-state properties. Among the Bose systems that have been studied with this method are hard sphere,[3] Yukawa[4] (a crude model of neutron matter), and Lennard-Jones[5] (a good model of ^{4}He). To our knowledge there have been no equivalent simulations of Fermi systems with more than four particles.

In this paper, we will show how the usual Metropolis method can be applied to sample the square of an antisymmetric wave function, and how the physical properties of the system can be calculated. We will base our variational calculations on wave function of the form

$$\psi(r) = \psi_J(r) D \ , \tag{1}$$

where ψ_J is a Jastrow or product wave function and D is a product of Slater determinants of single-particle wave functions. The trial wave function is adjusted to minimize the variational energy

$$E = \int dR\, \psi^*(R) H \psi(R) \Big/ \int dR\, |\psi(R)|^2 \tag{2}$$

where H is the Hamiltonian

$$H = -\frac{\hbar^2}{2m} \sum_i \nabla_i^2 + \sum_{i<j} V(r_{ij}) \ . \tag{3}$$

By the variational principle, this energy is an upper bound to the ground-state energy E_0 of the Schrödinger equation

$$H\psi_0 = E_0 \psi_0, \quad E \geq E_0 \ . \tag{4}$$

Other ground-state properties are also computed; their values are not stationary but are expected to be representative of the ground state if the trial wave function is good.

Direct sampling of the N-particle probability yields a rigorous upper bound to the energy; all other methods ultimately involve an expansion, and only the lowest-order terms can be evaluated. Although the systems we study here are quite simple, Monte Carlo methods lend themselves easily to more complex problems. In this paper we are only concerned with homogeneous systems of identical particles. With the same method one can simulate nonhomogeneous systems consisting of mixtures of particles with different masses, statistics, and interparticle potentials.

This paper is divided into two parts. First, we discuss the Monte Carlo algorithm: how one samples the square of a wave function of the form of Eq. (1) efficiently; how one calculates other properties of the system; and how one can best minimize the energy. In the second part, we apply to method to several physical problems: ^{3}He, several different models of neutron matter and Yukawa particles. The energies of these Fermi systems have been calculated by other authors using the Wu-Feenberg "perturbation" expansion. Recently,[4,6] however, doubts have been raised as to whether this expansion converges quickly enough to be of use in calculating the equation of state. Our calculations show that this approximation always underestimates the energy because the structure function is not accurately computed. We have computed the energies of both fluid and crystalline phases for a wide range of Yukawa potentials. The Yukawa system can be characterized by the single de Boer parameter $\Lambda^* = h/\sigma(m\epsilon)^{1/2}$. Our calculations show that if $\Lambda^* > 0.72$ then there is no crystal phase at any density. We have recently found a similar result for boson systems.

II. SAMPLING THE TRIAL WAVE FUNCTION

A. Wave function

In this paper, we are concerned with a homogeneous system of N identical particles in three dimensions with g spin states for each spatial state. The particles are placed in a cube with periodic boundary conditions in all three directions. We assume that in the ground state the g spin states are equally populated. Let the coordinates of the particles be $(\vec{r}, s)_i$ where s is the spin coordinate, $1 \le s \le g$, and $1 \le i \le I = N/g$. Then we assume the wave function is of the form

$$\psi(R) = \exp\left(-\sum_{i=1}^{N} \chi(\vec{r}_i) - \sum_{i<j}^{N} u(\vec{r}_{ij})\right) \times \prod_{s=1}^{g} d_s((\vec{r}, s)_i) \ , \tag{5}$$

where $\chi(r)$ is the single-particle pseudopotential, $u(r)$ is the two-particle pseudopotential, and d_s is a determinant

$$d_s = \det(D^s_{ij}), \quad D^s_{ij} = \Phi_j((r, s)_i) \ . \tag{6}$$

At this point we do not need to specify $u(r)$, $\chi(r)$, or Φ_i as nothing in the algorithm depends on special properties, except that they be readily computable.

B. Metropolis algorithm

The method of sampling the wave function is identical to that used for classical ensembles.[7] The only complication that arises is the evaluation of the determinant. Initial coordinates are chosen for each particle; typically they are either on a lattice or are a result of a previous Monte Carlo calculation. The particles are then moved one by one to new trial positions. Suppose particle 1 is being moved. Then its new trial position r_{new} is

$$\vec{r}_{\text{new}} = \vec{r}_1 + \vec{\xi} \ , \tag{7}$$

where $\vec{\xi}$ is a random vector uniformly distributed in a cube of side Δ centered at the origin. The new position for particle 1 is accepted with a probability equal to

$$P = \min[1, |\psi(r_{\text{new}})/\psi(r)|^2] \ . \tag{8}$$

If the absolute value of the wave function at the new position is larger than at the old, the new coordinates are automatically accepted. This random walk is Markovian and by the usual argument[1] the set of coordinates generated by a sufficiently long calculation is an unbiased sample drawn from the probability distribution

$$|\psi(R)|^2 \Big/ \int dR\, |\psi(R)|^2 \ .$$

The presence of nodes in the wave function will not affect the ergodicity of the random walk; the value of the step size Δ is large enough so the walk can easily jump over the nodal surface. In fact this is observed to happen frequently.

The expectation value of any operator F is simply the average value of the operator evaluated for the coordinates of the random walk with M moves

$$\langle F \rangle = \int dR\, \psi^*(R) F(R) \psi(R) \Big/ \int dr\, |\psi^2| \cong \frac{1}{M} \sum_{i=1}^{M} F(R_i) \ . \tag{9}$$

The most effective way to handle this wave function is to calculate the inverses of the matrices D^s at the beginning of the random walk and then update them as the particles are moved. This inverse is needed to compute the Metropolis acceptance ratio [Eq. (8)] and the variational energy. Let $\bar{D}^s$ be the inverse of the transpose of D^s of Eq. (6). Then, by definition,

$$\sum_{j=1}^{I} \bar{D}^s_{ij} D^s_{kj} = \delta_{ik} \ . \tag{10}$$

Note that the first index always represents an orbital, the second a particle. Now the determinant of a matrix is equal to the scalar product of any column (row) of the matrix with the same column (row) of the matrix of cofactors. Let particle 1 (with spin s) be moved to a new trial position [Eq. (7)]. Since only one particle is being moved; only one column of the matrix D^s will change, and the required ratio of wave functions is easily evaluated. Since $\bar{D}^s$ is proportional to the matrix of cofactors, the ratio of determinants is

$$\sum_{j=1}^{I} \bar{D}^s_{j1} \Phi_j(r_{\text{new}}) = q \ ,$$

and

$$\frac{\psi(R')}{\psi(R)} = q \exp\left(-\sum_{j=2}^{N} u(r'_{ij}) - u(r_{ij})\right). \tag{11}$$

If the move is accepted all of the elements of $\bar{D}^s$ need to be changed.

$$\bar{D}^s_{ji} = \begin{cases} \bar{D}^s_{ji}/q, & i = 1 \ , \\ \bar{D}^s_{ji} - \bar{D}^s_{j1} \sum_{k=1}^{I} \dfrac{\bar{D}^s_{kj} \Phi_k(r_{\text{new}})}{q} \ , & i \ne 1 \ . \end{cases} \tag{12}$$

It is easy to check that the new inverse matrix satisfies Eq. (10).

C. Energy estimation

The real utility of the inverse matrices $\bar{D}^s$ is in computing the average energy for a given trial

wave function. Since the particles are identical we need only consider the average energy of the first particle:

$$E_1 = V_1 + 2T_1 - F_1^2 , \tag{13}$$

where V_1 is the average potential energy,

$$V_1 = \left\langle \frac{1}{2} \sum_{j=2}^{N} V(r_{ij}) \right\rangle \tag{14}$$

and F_1^2, the mean square "pseudoforce,"

$$F_1^2 = \left\langle \frac{\hbar^2}{2m} (\vec{\nabla}_1 \ln\psi)^2 \right\rangle = \frac{\hbar^2}{2m} \left\langle \left| - \sum_j \vec{\nabla}_1 u(r_{1j}) - \vec{\nabla}_1 \chi(r_1) + \sum_{j=1}^{I} \bar{D}^s_{j1} \vec{\nabla}_1 \Phi(r_1) \right|^2 \right\rangle . \tag{15}$$

The average kinetic energy is the difference of two terms, $2T_1$ and F_1^2, where

$$T_1 = \left\langle -\frac{1}{2} \frac{\hbar^2}{2m} \vec{\nabla}_1 \cdot \vec{F}_1 \right\rangle = \left\langle \frac{\hbar^2}{2m} \nabla_1^2 \ln(\psi) \right\rangle . \tag{16}$$

There are several "Green's relations" which can be used to convert these averages to other forms. For example it is easy to show that the kinetic energy is equal to the mean square pseudoforce,[8]

$$T_1 = F_1^2 . \tag{17}$$

This relation is usually used to eliminate the pseudoforce in the energy (13). Another relationship is due to Feynmann[9]

$$\left\langle \frac{(\nabla_1^2 \psi_J d)}{\psi_J d} + |\nabla_1 \ln(d)|^2 - \frac{(\nabla_1^2 \psi_J)}{\psi_J} \right\rangle = 0 . \tag{18}$$

Using this we can transform the average energy to

$$E_1 = E_J + F_D^2 , \tag{19}$$

where E_J is the boson energy[10]

$$E_J = V_1 + \frac{\hbar^2}{2m} \left\langle \left(\sum_{j=2}^{N} \vec{\nabla}_1^2 u(r_{1j}) + \nabla_1^2 \chi(r_1) \right) \right\rangle - \frac{\hbar^2}{2m} \langle (\nabla_1 \ln\psi_J)^2 \rangle , \tag{20}$$

and F_D is the antisymmetric part of the pseudoforce

$$F_D^2 = \frac{\hbar^2}{2m} \left\langle \left(\sum_{j=1}^{I} \bar{D}^s_{j1} \vec{\nabla}_1 \Phi(r_1) \right)^2 \right\rangle . \tag{21}$$

However, there is a good reason not to use these transformed formulas for the energy. The variance of the original form [Eq. (13)] goes to zero as the wave function approaches an eigenstate of the Hamiltonian (This is strictly true only for the total energy $\sum_{i=1}^{N} E_i$). We have found that the variance of the transformed energies for simple Bose and Fermi problems is from 4 to 20 times larger than that of the direct form. To understand this consider the ideal gas. The direct form will give the correct answer at each step of the random walk, while the transformed form (19) is unbounded because the pseudoforce diverges at a nodal surface.

In a Bose calculation it is convenient to eliminate the pseudoforce from the energy, then the energy is an integral over the radial-distribution function $g(r)$. Hence, only $g(r)$ need be calculated by the Monte Carlo simulation and scaling[1] can then reduce the number of simulations needed to find the variational minima at different densities. The pseudoforce cannot be conveniently eliminated with a determinantal wave function, and we need to find other methods for quickly finding the variational minima. The additional computation needed to calculate the forces (about 20% in a Bose problem) is well worth the increased accuracy and reliability of the resulting energy. We use the two Green's relations as a check on convergence of the random walk, since they will be satisfied only if the entire configuration space is adequately sampled.

The pressure is computed from the virial theorem

$$P = \tfrac{2}{3} \rho \left[T_1 + \frac{1}{4} \left\langle \sum_j \left(-r_{1j} \frac{dV}{dr} (r_{1j}) \right) \right\rangle \right]. \tag{22}$$

It is known[11] that the virial pressure will be the same as the thermodynamic pressure $(-dE/dv)$ if the energies are evaluated at the variational minima. The consistency of these two quantities implies nothing about the closeness of the wave function to the ground state.

D. Energy minimization

We have used two methods to facilitate the search for the parameters of the wave function that give the minimum energy. These methods are different ways of finding the change in energy for a small change of parameters. The first method uses the technique of correlated sampling to find the effect of a small change of the variational parameters. One begins with the configurations generated by the Monte Carlo random walk for the wave function $|\psi_J D|^2$. Suppose we want to find the energy for the different Jastrow function $\psi_{J'}$ using these configurations. To do this use Eq. (13) with relationship (17) to eliminate the pseudoforce; the expressions for potential energy and the energy from the Slater determinant are unchanged. Use $|\psi_{J'}(R)/\psi_J(R)|^2$ as weights to calculate these energies. The variance of the relative energy $E_{J'} - E_J$ is much less than of the energy alone since the two energies are highly correlated. The weights must

be of the same order of magnitude if the answer is to be reliable so this method can be used only if $\psi_{J'}$ is near ψ_J.

The second method involves calculating the derivative of the wave function with respect to a parameter α. Since the Hamiltonian H is Hermitian, it is easy to show that

$$\frac{\partial E_1}{\partial \alpha} = \langle \Upsilon(R) E_1(R) \rangle - \langle \Upsilon(R) \rangle \langle E_1(R) \rangle \ , \tag{23}$$

where Υ and $E_1(R)$ are defined by

$$\Upsilon(R) = 2d \ln \psi(R)/d\alpha, \quad E_1(R) = H_1 \psi/\psi \ . \tag{24}$$

If ψ were the true ground state, then $E(R)$ would be spatially constant, and the estimate of $dE/d\alpha$ would have zero variance. Hence for good wave functions we expect this estimate of the derivative to be accurate. For example, suppose the pseudopotential $u(r)$ is proportional to α. Then $\Upsilon = -2u(r)/\alpha$ and the derivative of the energy with respect to α is the correlation between the total system energy and the pseudopotential. In this case, we can see that the variance of the estimate of the derivative is proportional to the number of particles for a large system. We can write the derivative as

$$\frac{\alpha dE_1}{d\alpha} = -2 \sum_{i<j} \langle u(r_{ij}) E_1(R) \rangle + 2 \sum_{i<j} \langle u(r_{ij}) \rangle \langle E_1(r) \rangle \ . \tag{25}$$

The contribution to the average comes mainly from pairs (i,j) close to particle 1, the particle singled out in Eq. (25). All of the other pairs contribute to the variance but not to the average value. Hence, in order to make this estimate accurate for a large system, these other pairs must be excluded from the sum.

E. Correlation functions

In this section, we define the two-particle correlation function, the structure function, the single-particle density matrix and the momentum-distribution function. The two-particle correlation function is the probability density that two particles will be separated by a certain distance. For a spin system the probability depends on the particles's relative spin. If $r_i\sigma_1$ and $r_j\sigma_j$ are the spatial and spin coordinates of two particles then the correlation function $g_L(r)$ for parallel spins is

$$g_L(\vec{x}_1, \vec{x}_2) = V^2 \left(1 - \frac{1}{N}\right) \times \langle \delta_{\sigma_i \sigma_j} \delta^3(\vec{x}_1 - \vec{r}_i) \delta^3(\vec{x}_2 - \vec{r}_j) \rangle \ . \tag{26}$$

The correlation function $g_U(r)$ for antiparallel spins is

$$g_U(\vec{x}_1, \vec{x}_2) = V^2 \left(1 - \frac{1}{N}\right) \times \langle (1 - \delta_{\sigma_i \sigma_j}) \delta^3(\vec{x}_1 - \vec{r}_i) \delta^3(\vec{x}_2 - \vec{r}_j) \rangle \ . \tag{27}$$

The total-correlation function is simply $g(r) = g_L(r) + g_U(r)$. For an infinite, homogeneous, isotropic system this function depends only on $r = |x_1 - x_2|$ and will go to a constant for large r.

The structure functions are Fourier transforms of the correlation functions. Let

$$\rho^s_{\vec{k}} = \sum_{i=1}^{N} \delta_{s\sigma_i} e^{i\vec{k} \cdot \vec{r}_i} \ . \tag{28}$$

The structure functions for parallel and antiparallel spins are then given by

$$S_L(\vec{k}) = \frac{1}{N} \sum_{s_1 s_2} \langle \rho^{s_1 *}_k \rho^{s_2}_k \delta_{s_1 s_2} \rangle = 1 + \rho \int d^3 r e^{i\vec{k} \cdot \vec{r}} \left(g_L(\vec{r}) - \frac{1}{g} \right) \tag{29}$$

and

$$S_U(\vec{k}) = \frac{1}{N} \sum_{s_1 s_2} \langle \rho^{s_1 *}_k \rho^{s_2}_k \, (1 - \delta_{s_1 s_2}) \rangle = \rho \int d^3 r \left(g_U(r) - 1 + \frac{1}{g} \right). \tag{30}$$

The usual structure function $S(k)$ is the sum of $S_L(k)$ and $S_U(k)$. In our computations we find the structure functions both by Fourier transforms of the $g(r)$ is and directly from the momentum coordinates $\rho^s_{\vec{k}}$.

The single-particle density matrix is a measure of the change in the wave function if a particle is displaced,

$$n(x_1, x_2) = \langle \delta^3(\vec{r}_1 - \vec{x}_1) \psi(x_2)/\psi(r_1) \rangle \ . \tag{31}$$

In a fermion system, because of the Pauli principle, there is no momentum condensate, and n must go to zero for large $|x_1 - x_2|$. For an infinite homogeneous system, n will depend only on $r = x_1 - x_2$ and in magnitude must be less than or equal to unity.[12] In contrast to a Bose system $n(x_1, x_2)$ can be negative.

The Fourier transform of this function is the probability density that a particle has momentum k

$$n(\vec{k}) = \rho \int d^3 r \, e^{i\vec{k} \cdot \vec{r}} n(\vec{r}) \ . \tag{32}$$

Assume that the coordinates of the Monte Carlo random walk and the inverse matrix $\bar{D}^s$ have been saved. Then we calculate these functions by randomly placing a new coordinate in the simulation cube.[1] The new particle at r' is assumed to have been displaced from one of the old particles (say r_1). Then

$$n(|r_1 - r'|) = \left\langle \exp\left(\sum_{j=2}^{N} u(r' - r_1) - u(r_1 - r_j)\right) \sum_{j=1}^{I} \bar{D}_j^s \Phi(r') \right\rangle \tag{33}$$

The momentum density can be calculated either as the Fourier transform of $n(r)$ or directly as

$$n(\vec{k}) = \langle e^{i\vec{k}\cdot(\vec{r}_1 - \vec{r}')} \psi(r')/\psi(r_1) \rangle \ . \tag{34}$$

F. Computational considerations

It is often stated[13] that it is not computationally feasible to sample the square of a fully antisymmetric wave function for a reasonably large number of particles—of the order of 100. Indeed a casual comparison of the storage and operational requirements of a Fermi and a Bose simulation suggests that a fermion computation will be much more costly. Storing the inverse matrix will require an additional N^2/g numbers. If a move is accepted, the number of operations needed to update this matrix is about $2I^2$. In an equivalent Bose calculation *without* neighbor tables, the amount of storage and the number of operations needed at each step of the random walk is proportional to N. If the potential is short range, then nearest neighbor tables can be used and the number of operations is proportional to the number of nearest neighbors. For such short-range systems it is possible to conduct simulations with several thousand particles.

While at the present time it would be difficult to simulate a Fermi system with thousands of particles, we have found it possible to do a system with over 100 particles. For such a system, the comparisons of computer time are deceptive since the operations involved in updating the inverse matrix are very simple and on most computers can be performed very quickly; computing the boson part of the wave function involves calculating periodic distances in three dimensions, and finding the pseudopotential and pseudoforce. We find that we can simulate a 114 particle Fermi system in only twice the time as a Bose system.[14] Much larger systems will require both a larger computer memory and more operations. With the present rate of computer evolution it will be possible to simulate much larger systems in the near future. The moderately large systems we have considered appear to be good representations of an infinite medium for many problems. In most cases we have estimated the size effect by performing calculation for systems having different N.

In the Metropolis algorithm, the step size Δ is a free parameter. Usually it is continually adjusted so that the acceptance ratio will be $\frac{1}{2}$. But for a fermion calculation, updating the inverse only needs to be done when a move is accepted, so that one can speed up the calculation by increasing Δ and thus decreasing the acceptance ratio to the range 10% to 30%. The information calculated for the rejected moves is not discarded. Suppose that $f(R)$ is a function to be averaged over all configurations. If R_{new} is a new set of trial coordinates, and P is the probability of accepting this new move from Eq. (8), then it is easy to show that the average value of f can be obtained by averaging the "expected" value of f,

$$\langle f \rangle = \langle P f(R_{\text{new}}) + (1 - P) f(R_{\text{old}}) \rangle \ . \tag{35}$$

The advantage of using this form is that some information about unlikely moves appears in the final answer, and hence the variance of f is lowered. As an example, the energy $E(R)$ diverges at a nodal surface, but since P goes to zero there [and $PE(R)$ goes to zero] the expected value is well behaved. The method of expected values is employed for all quantities which are averaged over the random walk-for example the energies, the structure function, the pressure. Coupled with the low-acceptance ratio this increases the efficiency of the computer program.

The propagation of round-off errors in the large inverse matrices $\bar{D}^s$ could be a problem. However the Slater matrices D^s are well conditioned since there is usually one element in each row and column close to unity, large density fluctuations are ruled out by the Jastrow wave function. Also a move near a node of the determinant, where the numerical error would be the largest, is rarely accepted. We have found that numerical inaccuracy is not a problem if arithmetic is done with 14 decimal digits, even when the matrices are updated 10^5 times.[15]

We have also investigated two other Monte Carlo techniques for calculating the energy of a determinantal wave function. They did not prove as satisfactory as the above method. The interested reader can find descriptions of them in Appendix A.

III. APPLICATIONS

The remainder of this paper will contain the results of the Monte Carlo algorithm applied to various physical systems with different potentials, Table I. We start by describing the various wave functions we have used. Then we take up each of the systems in Table I, present the Monte Carlo results, and discuss their relationship with previous calculations.

TABLE I. Potentials. Various interparticle potentials used. Here r is the radial separation and σ the spin. Λ^* is the "quantumness" parameter. For the Lennard-Jones potential it is defined as $\Lambda^* = [\hbar/\sigma(m\epsilon)^{1/2}]$. For a potential which behaves as r^{-1}, it is defined by $\Lambda^* = [\hbar\mu_e/(m\epsilon)^{1/2}]$, where ϵ and $\frac{1}{2}\mu_e^2$ are the coefficients of the terms in r^{-1} and r in the expansion of the potential about $r=0$.

Name	Potential	Λ^*	Symbol
Lennard-Jones	$4\epsilon[(\sigma/r)^{12} - (\sigma/r)^6]$; $\epsilon = 10.22\,^\circ$K $\sigma = 2.556$ Å	3.08 (^{3}He)	$P1$
Reid soft core	$V(r) = \begin{cases} (3.49f - 933.5f^4 + 4152.1f^6)/\mu r; & (\sigma_i = \sigma_j);\ f = e^{-\mu r} \\ (-3.49f - 1292f^4 + 2076f^6 + 3242f)/\mu r; & (\sigma_i \neq \sigma_j);\ \mu = 0.7/\text{fm} \end{cases}$	$1.20 (\sigma_i \neq \sigma_j)$ $\mu_e = 5.09$	$P2$
Reid $2p_3$	$V = (-10.463f + 105.468f^2 - 3187.8f^4 + 9924.3f^6)/\mu r f = \exp(-\mu r)$ $\mu = 0.71$ fm	0.89 $\mu_e = 4.69$	$P3$ $P4$
Yukawa	$\epsilon \exp(-\mu r)/r$	$\hbar\mu/(m\epsilon)^{1/2}$	
Homework	$V = \epsilon \exp(-\mu r)/r$; $\epsilon = 9263.1$ meV fm; $\mu = 4.9$/fm	0.93	$P5$

A. Wave functions

All of the wave functions used in our calculations have the form of Eq. (5). The various pseudopotentials and orbitals we used are shown in Table II. In most cases they are identical in form to ones used for the corresponding Bose problem.

We have used two different types of single-particle orbitals. For a liquid the orbitals were the plane waves of an ideal Fermi gas. The periodic boundary conditions restrict the plane waves to those with $\vec{k} = 2\pi\vec{n}/L$, where $\vec{n}$ is an integer vector. For the ground state, $\Phi_{\vec{k}}$ can be assumed to be real; sines and cosines were used. In order for the trial wave function to have all of the symmetries of the true ground state, we chose the particle number $N = gI$ so that a complete shell in k space would be filled. That is, I was chosen from the following sequence of numbers: 1, 7, 19, 27, 33, 57, ...

For a solid, the orbitals were Gaussians centered at a set of lattice sites. If the coordinates of a particle are r and s, its orbitals were $\exp[-c(\vec{r} - \vec{R}_i^s)^2]$ where $\vec{R}_i^s$ are the coordinates of a simple cubic sublattice. Each spin species has its own sublattice. For $g=2$, the total lattice is bcc with an antiferromagnetic ordering. If our simulation box is a cube, and $g=2$, we are restricted to 16, 54, or 128 particles.

A single-particle pseudopotential $\chi(r)$ ($W3$) was also used to localize the particles on lattice sites. This symmetric function was then multiplied by a Slater determinant of plane waves so that a fully antisymmetric function was obtained. This type of wave function, called "charge-density waves," has been proposed[16] as the ground state of "jellium." However for the soft-core Yukawa potentials the Slater determinant of Gaussian orbitals combines the energy of antisymmetrization and the energy of localization thus saving some energy. It may be that a more complicated $\chi(r)$, still having the periodicity of the lattice, would be a good ground-state wave function for some soft-core system.

The two-particle pseudopotentials $u(r)$ are also

TABLE II. Trial wave functions used in our calculations.

Component	Name	Function	Parameters	Restrictions	Symbol
$\varphi_{\vec{n}}(\vec{r})$	plane wave	$\cos\left(\frac{2\pi}{L}\vec{n}\cdot\vec{x}\right)$	$\vec{n}$	L = box edge $\vec{n}$ = integer vector	$W1$
		$\sin\left(\frac{2\pi}{L}\vec{n}\cdot\vec{x}\right)$		$2\pi/L\,\lvert n\rvert < k_F$	
$\varphi_n(\vec{r})$ or $\chi(\vec{r}_n)$	Gaussian	$\exp[-c(\vec{r} - \vec{r}_n)^2]$	c	$\vec{r}_n$ lattice vector $c(L/2)^2 \gg 1$	$W2$
$\chi(\vec{r})$	density wave	$\sum_{\vec{k}} C_k e^{i\vec{k}\cdot\vec{r}}$	$C_{\vec{k}}$	$\vec{k}$ a reciprocal-lattice of crystal	$W3$
$u(r)$	Mc Millan	$(b\sigma/r)^m$	bm $m = 4, 5$		$W4$
$u(r)$	Yukawa	$Ae^{-Br}(1 - e^{-r/D})/r$	A, B, D	These were smoothed (see text)	$W5$
$u(r)$	sine	$-2\ln[\sin(\pi r/2b)]\ r < b$ $0\ \ r > b$	b		$W6$

shown in Table II. The cutoff method was used in calculating all interparticle averages; if the distance between two particles was greater than $\frac{1}{2}L$ that pair was disregarded. It was found for the systems studied the two-particle correlation function $g(r)$ had reached its asymptotic constant value at $\frac{1}{2}L$, hence a tail correction could be used in calculating the potential energy and the pressure for $r > \frac{1}{2}L$. The pseudopotential $u(r)$ was altered so that it went smoothly to zero at $\frac{1}{2}L$. The wave function and its first derivative must be continuous in order for the energy to be a rigorous upper bound. *All* u's of Table II were smoothed by finding a point $r' < \frac{1}{2}L$ such that the polynomial $u_0(r - L/2)^3 + u_1$ matched $u(r)$ up to and including the second derivative at r'. Then, the altered pseudopotential $u'(r)$ we actually used was

$$u'(r) = \begin{cases} u(r) - u_1, & r \le r' , \\ u_0(r - \frac{1}{2}L)^3, & r' \le r \le \frac{1}{2}L , \\ 0, & \frac{1}{2}L \le r . \end{cases} \tag{36}$$

In practice, because of the continuity of the matching, the pseudopotential was little changed.

B. Ideal Fermi gas

As a test of our Monte Carlo algorithm, we sampled the square of the wave function for an ideal Fermi gas: the single-particle orbitals were plane waves, the pseudopotential was zero. The direct energy [Eq. (13)] is identically correct, but we verified the Green's relation Eq. (17) and computed the two-particle correlation function, and the structure function. These agreed with the known results within statistical errors.

The ideal Bose ground state is a trivial system with all of the particles in the zero-momentum state, and for this reason it shows no size dependence. On the other hand the ideal Fermi gas does have size dependence since as the number of particles increases, more and more shells in momentum space are filled. For this reason one might expect the size dependence of any Fermi system to be greater than that of the corresponding Bose system. Figure 1 shows the energy of the ideal Fermi gas, in periodic boundary conditions, as a function of the number of particles.

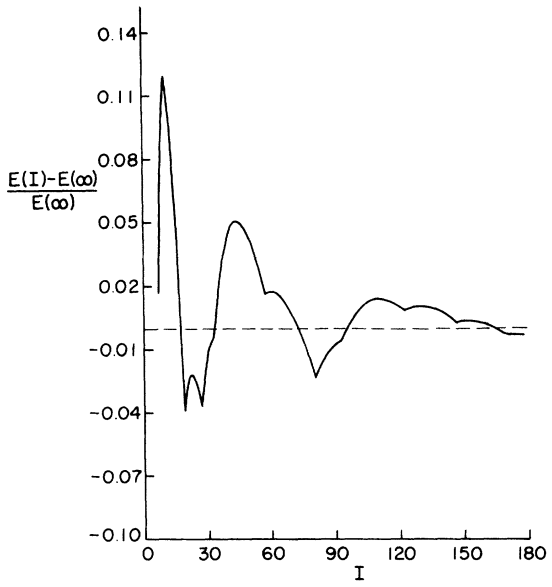

FIG. 1. Energy of an ideal Fermi gas as a function of I, the number of particles in a spin state.

C. Helium 3

Schiff and Verlet[2] have done a variational calculation for ^{3}He using Lennard-Jones potential ($P1$) in Table I, and the McMillan pseudopotential ($W4$) in Table II. They accounted for the Fermi statistics

TABLE III. Results of Monte Carlo computation for ^{3}He at three different densities and various particle numbers. N is the number of particles, b and c are the Jastrow parameters, V is the potential energy, T_D is the Slater kinetic energy, P is the pressure, and E is the energy (all in °K). γ is Lindemann's ratio (rms deviation from a lattice site divided by nearest-neighbor distance). B and F refer to a symmetric or antisymmetric wave function, respectively. L and S refer to a liquid or solid wave function, respectively.

System	Density	N	b	c	V	T_D	P	E	γ
					^{3}He				
$B\,L$	0.237	54	1.13	0	−11.50	0.0	0.31	−2.95 ±0.02	
$B\,L$	0.237	256	1.13	0	−11.52	0.0	0.17	−2.82 ±0.03	
$F\,L$	0.237	38	1.13	0	−11.59 ±0.15	2.34	−0.29 ±0.15	−1.34 ±0.07	
$F\,L$	0.237	54	1.13	0	−11.39 ±0.05	2.16	0.18 ±0.05	−1.31 ±0.03	
$F\,L$	0.237	114	1.13	0	−11.55 ±0.03	2.26	0.16 ±0.05	−1.20 ±0.03	
$B\,L$	0.414	114	1.145	0	−21.34 ±0.10	0	8.6 ±0.4	0.437 ±0.18	
$F\,L$	0.414	114	1.145	0	−21.35 ±0.13	3.20	9.0 ±0.4	2.84 ±0.06	
$B\,S$	0.427	864	1.092	2	−22.3 ±0.3	(7.386)	4.6	1.07 ±0.3	0.297
$F\,S$	0.427	54	1.092	2	−22.0	7.20	7.66	1.57 ±0.08	0.324
$F\,S$	0.427	128	1.092	2	−22.1 ±0.2	7.16	7.9 ±0.5	1.38 ±0.1	0.322

by using the Wu-Feenberg (WF) expansion[17] up to the second order. We have repeated their calculation at the density at which they obtained zero pressure ($\rho = 0.237/\sigma^3$) using exactly the same Jastrow parameters ($m = 5, b = 1.13$) for a 54 and for a 256 particle Bose system, and for 38, 54, and 114 particle Fermi systems. The results are shown in Table III. The Bose energies are in agreement with theirs, indicating that the size dependence of the energy is less than 0.1 °K. The fermion results are in fair agreement, the first-order energy of the Wu-Feenberg expansion being somewhat closer to our results than the second order. The change in energy in going from 54 to 114 particles

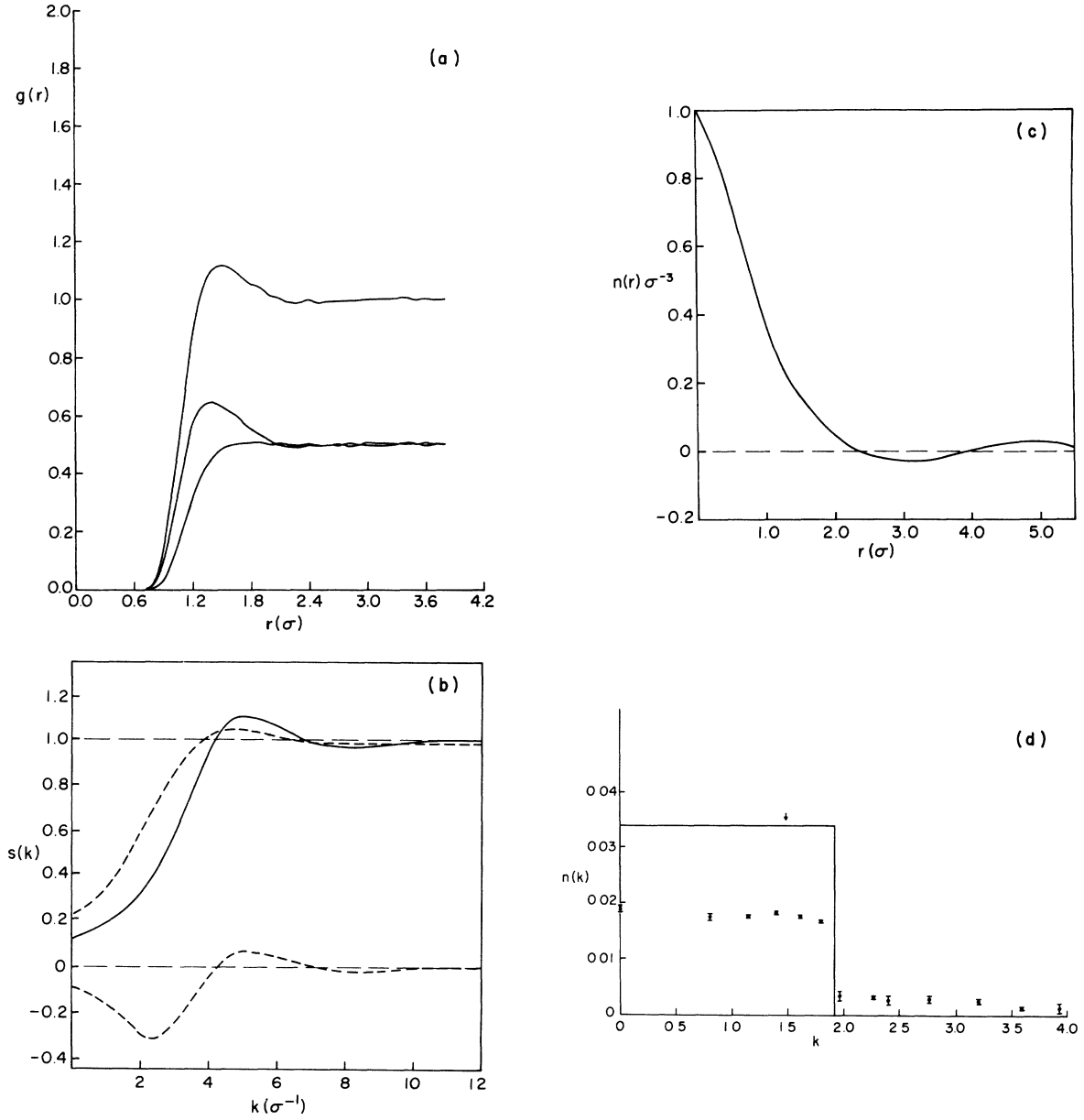

FIG. 2. (a) Radial-distribution functions of ^{3}He, for like spins $g_L(r)$, unlike spins, $g_U(r)$ and total $g(r)$. r is in units of σ, the density is $0.237/\sigma^3$. Upper curve $g(r)$ middle curve g_U, lower g_L. (b) Structure functions $S(k)$, $S_L(k)$ and $S_U(k)$ for ^{3}He; k is in units of σ^{-1}. Solid curve $S(k)$, dashed curve S_U, lower dashed S_L. Density is $0.237/\sigma^3$. (c) Single-particle density matrix, $n(r)$, for ^{3}He; r is in units of σ. Density is $0.237/\sigma^3$. (d) Momentum-distribution function, $n(k)$. The rectangle is the ideal-gas distribution for spin-$\frac{1}{2}$ fermions. The points are taken from our simulation of ^{3}He. The two arrows represent the rms values of k for the ideal gas and for ^{3}He. k is in units of σ^{-1}. $n(k)$ is normalized so that $\int d^3k\, n(k) = 1$. Density is $0.237/\sigma^3$.

is about 0.1 °K; judging from the Bose system, these two energies probably bracket the infinite system variational energy. Figure 2(a) shows the three distribution functions for this liquid (g, g_U, g_L). Note that the nearest neighbors to a given particle are usually particles of the opposite spin. The three-structure functions (S, S_U, S_L), are given in Fig. 2(b), the single-particle density matrix $n(r)$, in Fig. 2(c). Figure 2(d) shows the momentum-distribution function $n(k)$. The points are direct evaluations of $n(k)$ along several directions.[18] The effect of the Jastrow wavefunction is to excite 50% of the particles above the Fermi level, the sharp edge at k_F remains—a much larger system would be needed to see this function in detail. The rms value of k (proportional to the total kinetic energy) is $2.7/\sigma$ (compare this to $1.4/\sigma$ without the Jastrow factor.) Pandharipande and Bethe[19] have used a variational method based on the hypernetted chain (HNC) equation to calculate the energy of this problem. The antisymmetry is again handled by a permutation expansion. For a spherically symmetric Jastrow factor $u(r)$, they get −2.99 °K (Bose statistics) and −1.30 °K (Fermi statistics). However when they allow the correlation function to depend on relative momentum and spin, they get a lower energy (−1.97 °K). When we choose a pseudopotential which depends on the relative spin of the two particles

$$u_{\sigma_i\sigma_j}(r_{ij}) = u(r_{ij}, b)\left[1 + \delta_{\sigma_i\sigma_j}(\beta - 1)\right] , \qquad (37)$$

we find no significant lowering of the energy (less than 0.1 °K). This is true because the determinants have already separated like spins and the energy is insensitive to the pseudopotential between them.

Table III also contains our results for both Bose and Fermi liquid ^{3}He at the crystalization density $(\rho = 0.414/\sigma^3)$. Here, the first-order WF approximation underestimates the energy by 1.1 °K. This inaccuracy will effect the published estimates[20] of the liquid-solid transition density from variational calculations, pushing it to lower densities.[21]

Hanson and Levesque[20] have calculated the energy of solid bcc ^{3}He using a Jastrow function with Gaussian localization but without antisymmetrization. We have repeated this calculated with identical parameters $(\rho = 0.427/\sigma^3,\ b = 1.092,\ c = 2.0)$, changing the product of Gaussians to a determinant of Gaussians. The results are in Table III. The energies are in good agreement; our Fermi energy is two standard deviations higher than theirs, (about 0.3 °K). The density is quite close to the melting density but the particles are still localized. A pair of particles interchanged lattice sites once in 2×10^5 steps of the random walk. Lindeman's ratio γ, defined as the ratio of rms deviation from a lattice site to the nearest-neighbor distance, is 0.32. Both this ratio and the pressure are larger than the values of Hansen and Levesque. It appears that the pressure and γ are sensitive to the antisymmetrization of the Gaussian orbitals.

D. Neutron matter

The other systems that we have studied have soft-core potentials, of the type used to model neutron and nuclear matter. Recently there have been a number of calculations concerning the equation of state and solidification of neutron matter in the interior of neutron stars. Different techniques yield widely varying values for the solidification density of neutron matter,[13] from a density of 0.3 neutrons/F^3 to no solidification at all.[11] For a review, see Baym.[22] The calculations we will describe are not realistic models of neutron matter since the potential between neutrons is not accurately known for small separations, and a nonrelativistic treatment is clearly not adequate if the kinetic energy is a significant fraction of the rest mass. Nonetheless, accurate variational calculations are likely to provide some guidelines for the convergence of the expansions that are used in other treatments of this problem.

E. Nosanow and parish model of neutron matter

Nosanow and Parish[13] have assumed that the potential between two neutrons in a singlet state is the Reid soft core $^1S_0$; in a triplet state they use the central part of the $^3P_2$ potential. They have done a Monte Carlo calculation with a symmetric wavefunction and two pseudopotentials: the McMillan function with $m = 4$ ($W4$), and the sine function ($W6$). For the solid phase they used the Gaussian $\chi(r)$, ($W2$). They used the WF expansion up to first order in the liquid phase. In the solid phase they used an expansion based on the van Kampen cluster method.[23] A liquid-solid phase transition was found at a density of 0.3 to 0.45 neutrons/F^3.

To test the convergence of the WF expansion we have repeated their calculation at one density, 0.3 neutrons/F^3. The potential is $P2$ in Table I. Using the same pseudopotentials we find the results given in Table IV. Since like spins must be in a triplet state, they interact with a Reid soft core $^3P_2$. On the other hand, it is equally likely for unlike spins to be in either a triplet or singlet state; they therefore interact with the average of the $^1S_0$ and $^3P_2$ potentials. We find that the WF expansion consistently underestimates the energy by 15 to 30 MeV. The error is greatest for the soft sine Jastrow function ($W6$) where most of the error comes from the potential energy term. Later, it will be shown that this is a general characteristic of the WF expan-

TABLE IV. Results for the Monte Carlo simulation for potential $P2$, at a density $\rho = 0.3$ neutrons/F^3 in both the liquid and solid phase. The results marked MC are ours, those marked WF are from Ref. 12 and calculated using the Wu-Feenberg expansion. N is the number of particles b, c, A, B, D are variational parameters (see Table II). V, T_J, T_D, and E are the various energies in MeV. γ is Lindemann's ratio.

Method	Wave function	N	b	c	V	T_J	T_D	E	γ
MC	$W4$	54	0.425	0	−21.7	28.5	48.4	55.2 ± 0.8	···
MC	$W4$	114	0.425	0	−21.3	28.4	47.9	55.0 ± 0.6	···
WF	$W4$	···	0.425	0	−38.0	25.9	53.1	41.0	···
MC	$W4$-$W2$	54	0.45	0.40	−25.7	30.8	44.4	49.5 ± 1	0.555
MC	$W4$-$W2$	128	0.45	0.40	−26.4	30.2	62.9	66.7 ± 0.6	0.517
WF	$W4$-$W2$	···	0.45	0.40	−55.7	27.6	67.3	39.2	···
MC	$W6$	54	1.11	0	−29.3	39.2	57.6	67.5 ± 0.6	···
WF	$W6$		1.11	0	−41.4	27.6	50.8	35.3	···
			A	B D					
MC	$W5$	54	2.1	1.6 0.5	−26.1	30.3	45.5	49.7 ± 0.8	···

sion. Table IV also contains results obtained for the Nosanow-Parish model with the Yukawa trial function ($W5$). The energy is only slightly lower, indicating that the energy is not too sensitive to the two-body trial function. Note that the energy of the solid increases by 15 MeV when the system is changed from 54 particles to 128 particles. This is a result of the discontinuity of the first derivative in the Gaussian orbital at the edge of the box. To get a rigorous upper bound one must smooth the orbitals as was done with the pseudopotential. The localization of this crystal is very weak. Lindemann's ratio is 0.517. For a homogenous liquid it would be 0.577.[24] It is highly unlikely that a crystal with this localization would be stable. Indeed, we find that this crystal wave function has a higher energy than the liquid.

F. Spin-independent Reid potential ($^3S_1 - {}^3D_1$)

Recently, Pandharipande *et al.*[25] have compared the hypernetted chain variational (HNCV) method with the Brueckner-Bethe-Goldstone (BBG) expansion for several nuclear matter potentials. Surprisingly, the HNCV method gives energies lower by about 10 MeV at nuclear matter densities, for two different Reid potentials. This disagreement is quite serious since it casts doubt on the widely accepted BBG method of finding the ground state of nuclei, as well as the conventional models of two particle nucleon interaction. Using the Yukawa-Jastrow function ($W5$) we have calculated the variational energy of one of these potentials, the central part of the Reid ($^3S_1 - {}^3D_1$), at three densities in the liquid state for bosons (labeled $g = \infty$), neutron matter ($g = 2$) and symmetric nuclear matter ($g = 4$). The variational parameters we used and the results are shown in Table V.

The Bose fluid calculations made with HNCV are indistinguishable from our Monte Carlo results over this density range, a result that has been noted for other Bose fluids.[4,26] The lowest-order-Brueckner-theory (LOBT) energy[25] is quite good for densities less than 0.4 neutrons/F^3. Above

TABLE V. The result of the Monte Carlo simulation for potential $P3$ at three densities (in neutron/F^3) in the fluid phase. The wave function was Yukawa ($W5$), N is number of particles, and A, B, D are the variational parameters (in F). V, T_J, T_D, and E are the various energies in MeV. P is the pressure and E_{HNC} is from Ref. 18.

ρ	g	N	A	B	D	V	T_J	T_D	P	E_{HNC}	E
0.182	∞	54	1.5	1.4	0.15	−41.0	22.1	0	−2.4	−17.3	−17.7 ± 1
0.182	2	54	1.7	1.6	0.1	−44.5	22.3	31.3	−0.6	···	12 ± 0.4
0.182	4	108	1.7	1.6	0.1	−42.3	23.08	21.34	−0.2	−1.7	1.9
0.386	∞	54	2	1.7	0.08	−93.1	62.8	0	−2.6	−28.7	−30.2 ± 1
0.386	2	54	2	1.7	0.08	−98.1	60.9	57.12	6.6	···	17.3 ± 1
0.386	4	108	2	1.7	0.08	−94.0	61.9	34.4	4.7	−6.4	3.4 ± 5
0.822	∞	54	3.3	2.7	0.25	−150	14.9	0	100	0.0	−1.6 ± 2
0.822	2	54	3.3	2.7	0.25	−160.0	140.0	80	129	···	60 ± 2
0.822	4	108	3.3	2.7	0.25	−147	141.1	60.1	139	22.0	54.5 ± 5

that it rapidly becomes too small indicating that the approximation is breaking down. Unpublished results[6] of the next higher order of BBG completely remove the disagreement for bosons between BBG and HNCV at low densities.

However, for the fermion nuclear fluid ($g=4$) the different methods give different answers. Our energies are higher than those obtained using HNCV, but lower than those using LOBT. The disagreement seems to be roughly proportional to density. There are two plausible explanations for this discrepancy. First the class of wave functions over which the energy is minimized in HNCV is larger than with our variational calculation. The HNCV correlation function in a Fermi fluid can depend on the relative angluar and linear momentum of the two particles. (When this additional freedom is introduced into HNCV in calculating ^{3}He binding energy, the energy drops by 0.6 °K.[19]) For this nuclear matter potential we have also tried using the spin dependent u in Eq. (37), and again we found no significant drop in the energy. Since only $\frac{1}{4}$ of the other particles in the fluid have the same spin, and they are kept apart by the Pauli principle it is very unlikely that a spin-dependent pseudopotential could ever be important for a spin-independent interaction. A more likely candidate for the disagreement is the permutation expansion used in the HNCV approximation. The convergence of this expansion has never been tested, particularly for soft-core Jastrow functions and soft-core potentials. We discuss this at greater length below.

G. Repulsive Yukawa potential with $\Lambda^* = 0.93$ (potential $P5$, Table I)

A number of other workers[4,27] have calculated the liquid and solid properties of the potential $P5$.[28] There is now agreement that both the Bose and Boltzmann systems with this potential will not crystallize. We have found that a Fermi system with this potential also does not crystallize. In our work the Yukawa Jastrow function ($W5$) was used. The variational parameters and results are given in Table VI. Table X shows that the results of the first-order WF approximation always lie below the variational energy, the difference being much larger at high densities. Figure 3(a) shows the three distribution functions for this fermion liquid at nuclear matter density; Fig. 3(b) shows the three structure functions. Figure 3(c) gives the single-particle density matrix, Fig. 3(d) the momentum distribution function. These functions show a much more gaslike behavior than those for liquid ^{3}He at its equilibrium density. The edge of the momentum distribution at the Fermi wave vector remains but only 23% of the particles have been excited above it.

H. Yukawa fermions

The potential $P5$ is an example of a broader class of potentials of the Yukawa form, ($P4$). These potentials can be characterized by two dimensionless parameters: the DeBoer "quantumness" parameter Λ^*, and r_s, familiar from the electron gas,[16]

$$\Lambda^* = \left(\frac{\hbar^2\mu^2}{m\epsilon}\right)^{1/2}, \quad r_s = \frac{\epsilon m}{\hbar^2}\left(\tfrac{4}{3}\rho\right)^{-1/3}. \tag{38}$$

In the limit $\mu \to 0$, we expect this system to behave like an electron gas. For the Bose ground state, we have mapped out the phase diagram variationally in the (r_s^{-1}, μ) plane. In this plane, lines of constant potential or Λ^* are hyperbolas in which $(1/r_s)\mu \propto \Lambda^*$. We have checked the variational results with an exact Monte Carlo calculation which will be published elsewhere. With the knowledge of the boson phase diagram we were able to select a few points of r_s and Λ^* and locate roughly the Fermi liquid-solid phase line.

TABLE VI. Potential $P5$ fermions (liquid). Results of the Monte Carlo simulation with potential $P5$ for neutron matter ($g=2$) at 5 densities (in units of Neutrons/F^3) in the fluid phase. N is the number of particles A, B, D are the variational parameters for the Yukawa wave function $W5$ in F. E_{st} is the static (Madelung) energy of the fcc lattice, P is the pressure, E_B is the Bose energy, and V, T_J, and E are the energies. Energies are given in MeV, distances in F.

ρ	N	A	B	D	E_{st}	E_B	P	V	T_J	E
0.17	54	2.0	1.0	0.1	1.35	63.2	16.9	27.6	31.8	88.5 ± 0.6
0.17	114	2.0	1.0	0.1	1.35	63.2	16.4	26.2	31.7	89.6 ± 0.7
0.3	54	2.8	1.0	0.35	9.09	138	61.8	66.5	66.8	174.9 ± 0.7
1.0	54	2.7	2.0	0.30	214.5	726	1 039	519	166.7	782 ±2
2.0	54	2.5	2.1	0.19	886.1	1860	5 160	1452	385.5	1976 ±6
4.0	54	2.0	2.8	0.15	2981	4730	25 451	4068	599.4	4897 ±7
4.0	114	2.0	2.8	0.15	2981	4730	25 655	4077	597.2	4909 ±2

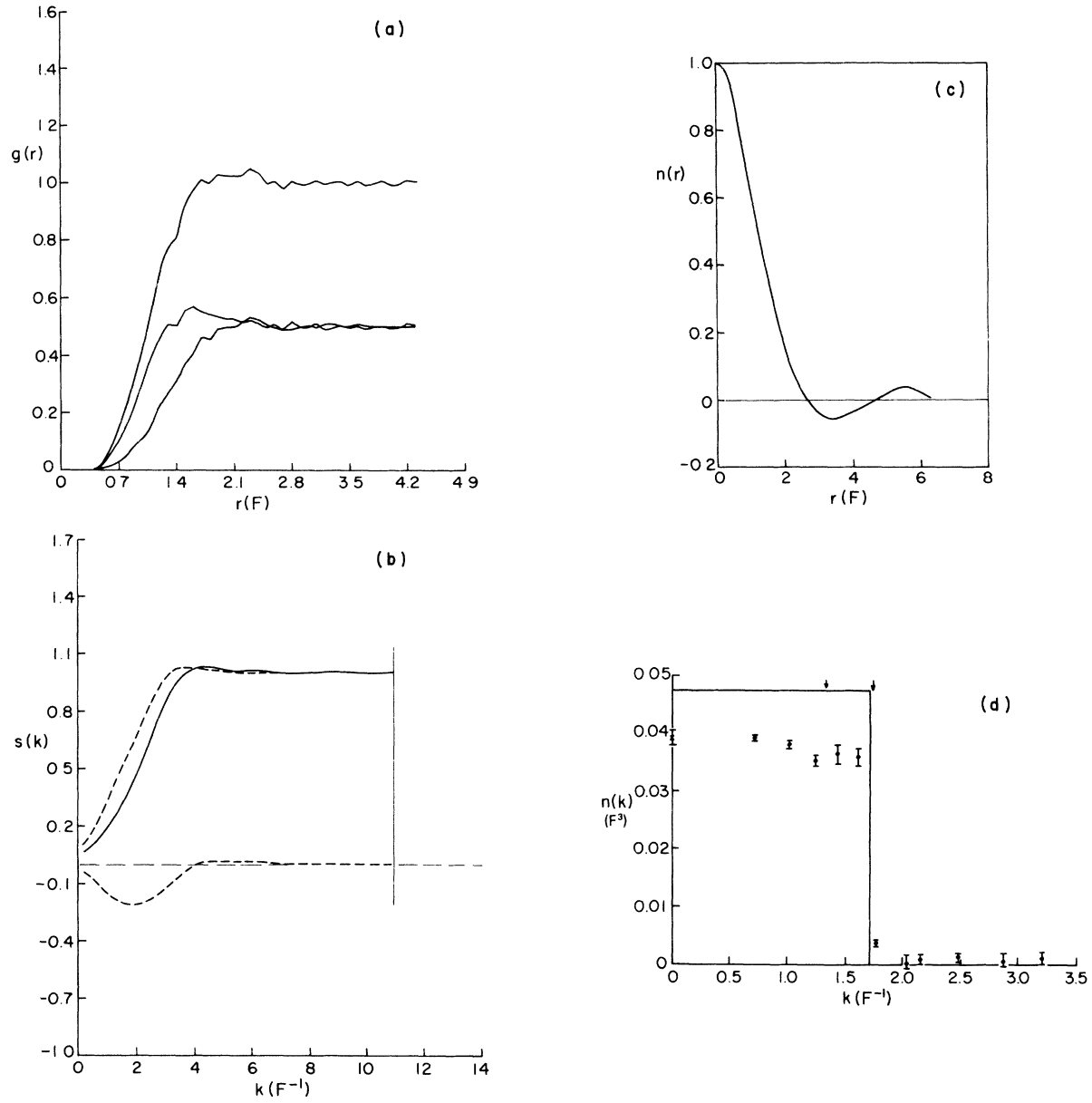

FIG. 3. (a) Radial-distribution functions g_L, g_U, and $g(r)$ for neutron matter at a density 0.17/Fm^3. r is in units of fermis. Upper curve $g(r)$, middle curve g_U, lower curve g_L. Density is 0.17/Fm^3. (b) Structure functions S_L, S_U, and $S(k)$ for neutron matter; k is in units of Fm^{-1}. Solid curve S, dashed curve S_U, lower dashed curve S_L. Density is 0.17/Fm^3. (c) Single-particle density matrix, $n(r)$, for neutron matter. r is in units of Fermis. Density is 0.17/Fm^3. (d) Momentum-distribution function, $n(k)$. The rectangle is the ideal-gas distribution for spin-$\frac{1}{2}$ fermions. The points are taken from our simulation of neutron matter. The two arrows represent the rms values of k for the ideal gas and for neutron matter. k is in units of Fm^{-1}. $n(k)$ is normalized so that $\int d^3k\, n(k) = 1$. Density is 0.17/Fm^3.

The Yukawa function ($W5$) was used for the pseudopotential. In the solid the single particle orbitals were Gaussians ($W3$), with the bcc antiferromagnetic ordering. Spot checks with the density-wave pseudopotential ($W3$) plus plane-wave orbitals ($W1$) produced higher eneriges. The phase diagram we found is shown in Fig. 4. The energies and variational parameters are given in Tables VI–VIII. In Tables VII, VIII the units of length are such that the density is unity, and the units of energy are such that $\hbar^2/2m$ is unity. We are limited to comparatively large values of μ because of the slow decrease of the potential. As discussed earlier, the potential and pseudopotential outside

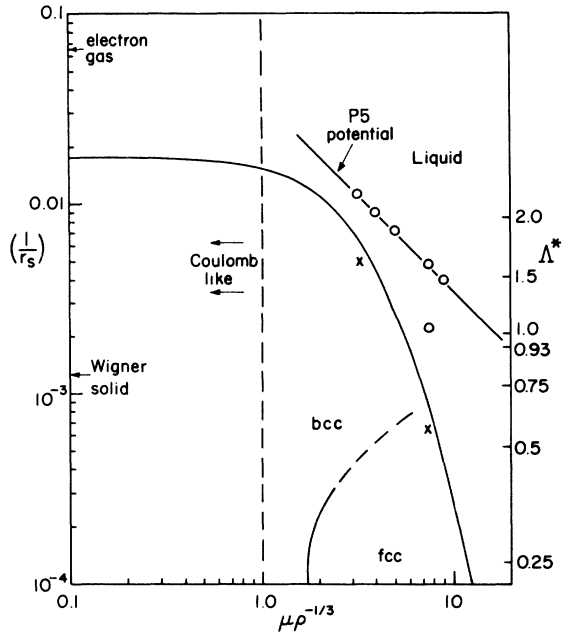

FIG. 4. Phase diagrams for the ground state of the Yukawa potential as found in our variational calculations. μ, r_s, and Λ^* are defined in the text. The circles are points which we found to be in the liquid phase, the ×'s are in the solid phase. The phase line is from the Gaussian model.

the simulation cube is only taken into account in an average way. If important correlations are not to be missed, the "Ewald image" method,[29] or an equivalent, would have to be used to study Yukawa systems for small values of μ.

The topology of the phase boundary is probably correct, but the actual position is somewhat in doubt. Consider a point in the crystal phase. As the density is increased along a line of fixed Λ^*, the system eventually becomes Coulomb-like, and since the high density phase of "jellium" is gas, the phase boundary must eventually bend over and touch the line $\mu = 0$. In other words, any Yukawa system compressed enough will pressure-melt. On the other hand, if the density is decreased along the same Λ^* line, the potential energy will go to zero exponentially fast, and the kinetic energy will eventually dominate. Hence, any Yukawa solid will melt if allowed to expand. If one fixes μ and goes to very large values of r_s, (or lets $h \to 0$) one would eventually expect to have a classical solid, since the kinetic energy would go to zero. For small μ the classical system prefers a bcc lattice,[30] at $\mu = 1.72$ there is a phase transition (which we find to have a width $\delta\rho/\rho = 1.2 \times 10^{-5}$) to the close-packed (fcc) lattice. One would expect spin-$\frac{1}{2}$ fermions to favor the bcc lattice since nearest neighbors then have different spins. Accordingly, we have drawn a tentative phase line curving sharply to the right.

The liquid-solid line in the vicinity of the points marked X was calculated by interpolating between the variational energies of the liquid and solid phases. Outside that region, the phase boundary is extrapolated by following a contour of constant Lindemann's ratio as predicted by the Gaussian model[31] of a Boltzmann solid. This procedure can be partially justified because within the region we have simulated the phase boundary lies on one of these contours, as it does for bosons. The Gaussian contour we have chosen characterized by is $\gamma = 0.147$. However, Lindemann's ratio for the Jastrow wave function is about 0.3. γ is much smaller in the Gaussian model since the particles must be tightly bound to the lattice sites to make up for the absence of two-particle correlations to keep them apart. In addition, we find that between 1% and 3% of the Wigner-Seitz cells are vacant. We believe the ground state may contain some delocalized vacancies. This question is being investigated in detail for the Bose ground state.

This work gives a rough guide to where the electron gas or "jellium" crystallizes, namely $r_s = 56$. Other estimates for the Wigner transition vary widely,[16] from $r_s = 5$ to $r_s = 700$. Our estimate for r_s probably gives a lower bound to the transition value of r_s because the variational wave function

TABLE VII. Yukawa fermions (liquid). Results of Monte Carlo simulations with the Yukawa potential ($P4$) and pseudopotential ($W5$) for a liquid. Λ^* and $1/r_s$ are dimensionless parameters which characterize the potential. μ is the potential curoff. Units of length are chosen so that the density is unity. A, B, and D are the variational parameters, N is the number of particles (spin-$\frac{1}{2}$), P is the pressure, V is the potential energy, T_D is the Slater kinetic energy, and E_F is the total energy. The units of energy are such that $\hbar^2/2m$ is unity.

Λ^*	$\mu\rho^{1/3}$	$10^3 r_s^{-1}$	A	B	D	N	P	V	T_D	E_F
0.628	3.24	4.97	4.2	1.6	0.1	54	55.4	141.5	4.48	164.6 ±0.1
0.344	7.43	0.65	3.1	1.8	0.04	54	3.60	29.9	5.30	48.26±0.04
0.628	7.33	2.2	2.2	2.3	0.1	38	1.73	13.7	4.45	25.9 ±0.1
0.628	7.33	2.2	2.2	2.3	0.1	54	1.83	13.1	5.08	25.9 ±0.1
0.628	7.33	2.2	2.2	2.3	0.1	114	1.73	13.6	5.18	26.5 ±0.2

TABLE VIII. Yukawa fermions (solids). Results of Monte Carlo simulations with a Yukawa potential (*P*4), and pseudopotential (*W*5) for a solid. The orbitals were Gaussians centered about bcc lattice sites. C is the Gaussian localization, γ is Lindemann's ratio, and V_0 is the probability that a Wigner-Seitz cell will be vacant. See the caption of TABLE VII for the definitions of other symbols and units.

μ	$10^3\times r_s^{-1}$	A	B	C	D	N	P	V	T_D	E_F	γ	V_0
4.90	7.20	2	2.7	3.0	0.5	54	55	28.91	9.14	41.41 ± 0.2	0.384	
3.88	8.95	2.9	2.2	2.5	0.25	54	127	43.8	7.88	60.44 ± 0.01	0.379	
3.08	11.42	3.2	1.8	1.6	0.24	54	307	30.55	5.67	94.2 ± 0.1	0.418	
3.24	4.97	3.4	1.8	5.3	0.17	54	54.6	134	16.1	162.7 ± 0.1	0.288	0.012
7.33	2.2	1.75	2.3	5.3	0.13	54	1.73	8.94	15.0	29.8 ± 0.4	0.314	0.031
7.43	0.65	2.15	1.86	4.3	0.04	54	3.42	25.9	13.1	47.6 ± 0.2	0.320	0.034
7.43	0.65	2.15	1.86	4.3	0.04	128	3.44	25.9	13.0	47.8 ± 0.6	0.324	

for the solid is probably "better" than the liquid one. We have found this to be true for the equivalent boson Yukawa system, the variational phase line lying at higher values of Λ^* than the exact phase line. The critical Lindemann's contour at very large values of μ obeys the equation

$$(1/r_s)\mu_c^2 = 0.0022 \ . \tag{39}$$

In retrospect, the widely varying values[22,27] of the crystallization density of neutron matter found in other calculations can be traced to this phase diagram. The energy of soft-core potentials, after the static energy is removed, varies slowly as a function of r_s and Λ^*. Furthermore, the energies of the liquid and solid phases are very close throughout this range of r_s. Hence it is easy for various approximations to place a Yukawa or Coulomb system in either the liquid or solid phase. Recently, Glyde *et al.*[32] have estimated that the Fermi one component plasma will melt at $r_s \simeq 70$. This estimate is fairly close to our own. It is however based on using the Wu-Feenberg expansion to estimate the effect of the Fermi statistics on the Bose system.

According to our variational calculations, unless a system has $\Lambda^* < 0.72$ it can never form a solid at zero temperature. The values of Λ^* for the other potentials are shown in Table I. These values were estimated for the other potentials: ϵ and μ are found by equating the terms proportional to $1/r$ and r in the small r expansion of the potential to the corresponding terms in the Yukawa potential. Most neutron matter potentials have $\Lambda^* \approx 1$.

I. Convergence of the Wu-Feenberg expansion

Recently Brandow[6] has argued that the Wu-Feenberg[17] expansion does not converge well enough to be useful. According to his argument, the effect of the exclusion principle is spread out over all orders of the permutation expansion. Hence, for an N particle system, the first order term only contains $\sim 1/N$ of the effect of the exclusion principle. The simulations we have done allow us to test the convergence, we will concentrate on the first order, since it should account for most of the antisymmetrization energy, if the series converges.

The energy of the wave function $\psi_J D$ can be split into three terms; the potential energy V, the kinetic energy arising from the Jastrow factor T_J, and the kinetic energy arising from the Slater determinant T_D. V and T_J can be expressed as integrals over the radial distribution function:

$$V = (\tfrac{1}{2}\rho/2)\int d^3r\, g(r) v(r) \ , \tag{40}$$

$$T_J = (\tfrac{1}{2}\rho/2)\int d^3r\, g(r) \frac{\hbar^2}{2m} \nabla^2 u(r) \ . \tag{41}$$

The remainder of the energy T_D [Eq. (15)] is

$$T_D = -(\hbar^2/4m)\langle \Delta_1^2 \ln D \rangle \ . \tag{42}$$

In the first order of WF, one keeps terms from the determinant involving only pair permutations. The two-particle correlation function is thus approximated by

$$g'(r) = g_B(r) g_{HF}(r) \ , \tag{43}$$

where $g_{HF}(r)$ is the free-fermion pair-correlation function

$$g_{HF}(r) = 1 - \frac{1}{2}\left(3 \frac{\sin k_F r - k_F r \cos k_F r}{(k_F r)^3} \right)^2 \ . \tag{44}$$

Here, $g_{HF}(r)$ is the ideal-gas correlation function and g_B is the correlation function arising from ψ_J. Then to first order in permutations the energies V and T_J are given by (40) and (41) with g replaced by g' and T_D is given by

$$T_D' = \frac{3}{5}\frac{\hbar^2}{2m} k_F^2 \left(1 - 20 \int_0^1 y^4\, dy [\, S_{HF}(2k_F y) - 1\,] \times [\, S_B(2k_F y) - 1\,] \right) .$$

S_{HF} is the free Fermi structure function

TABLE IX. First-order Wu-Feenberg energies and their deviations from variational results for ^{3}He at two densities. A prime indicates a WF result. V is the potential energy, T_J the Jastrow kinetic energy, T_D the Slater kinetic energy, and E the total energy (all in °K) S_0 is the structure factor at $k=0$, $\mathcal{E}$ the average Pauli condition (see text).

ρ	V'	$V-V'$	T'_J	$T_J-T'_J$	T'_D	$T_D-T'_D$	E'	$E-E'$	S'_0	$\mathcal{E}$
0.237	−10.95	−0.60	7.29	0.81	2.32	−0.07	−1.34	0.14	−0.68	1.70
0.414	−21.09	−0.26	19.61	1.38	3.25	−0.05	1.77	1.07	−0.61	3.27

$$S_{\mathrm{HF}}(k)=\begin{cases}\frac{3}{2}y-\frac{1}{2}y^3, & y<1,\\ 1, & 1<y,\end{cases}\qquad y=k/2k_F\ . \tag{45}$$

The structure function in the first-order WF expansion is given by

$$S'(k)=S_B(k)+12\int_0^1 y^2\,dy\,[S_{\mathrm{HF}}(2k_Fy)-1]\times[S_B(2k_Fy)-1]\ . \tag{46}$$

Schiff and Verlet[1] have found that the energies of the successive WF orders seem to converge rapidly for ^{3}He. However, the energies V, and T_J do not converge nearly as well. Table IX gives the results of the WF expansion to first order for ^{3}He at two densities. The lower density is very close to the zero pressure liquid, the higher is in the two phase region of liquid and solid. At zero pressure the errors in T_J and V, about 0.7 °K, nearly cancel out, so the energy as predicted by WF approximation is close to the variational value. At the higher density this cancellation does not take place, and the total energy is underestimated by 1.1 °K. Although this is only a small fraction of either the kinetic or potential energies, about 20 °K, the first-order WF expansion has only given half of the antisymmetrization energy. This error comes only from V, and T_J, the kinetic energy T_D is given accurately.

Table X gives the result of the WF expansion applied to the "homework" potential with $g(r)$ computed from the symmetric wave function ($W5$). Here again the kinetic energy arising from the Slater determinant, T_D, is given accurately; while the terms dependent on $g(r)$ are underestimated, the error seems roughly proportional to density. One can understand this to some extent by considering the structure factor at $k=0, S_0$. The structure factor for all of the wave functions in this paper is positive for *all* k. (The *exact* structure factor is zero at $k-0$ because of the phonon spectrum.) Tables IX and X contain S'_0 as calculated with Eq. (46). It is negative between −0.6 and −0.7 for both the potential $P5$ and ^{3}He and is almost independent of density. This problem with $S(k)$ has been noted by other authors.[33] Transforming the energy integrals over g to ones over S, one finds

$$V+T_J=\frac{1}{2\rho(2\pi)^3}\int d^3k\left(V(k)+\frac{\hbar^2}{2m}\,k^2u(k)\right)\times S(k)+\mathrm{const}\ . \tag{47}$$

Assume the error in $S(k)$ is concentrated in the region $k<\rho^{1/3}$ and is roughly constant there. Then very roughly, the error in the energy will be proportional to the scattering amplitude of the potential times the density.

$$E-E'_{\mathrm{WF}}\approx 0.65\rho\int d^3r\,\frac{v(r)}{12\pi^2}\ . \tag{48}$$

This accounts for the order of magnitude of the errors of WF for the "homework" potential. The dependence will be more complicated for ^{3}He since the Fourier transforms do not exist.

It is likely that T_D will be accurately given by the WF expansion for any dense fluid. This is because T_D depends only on the structure functions S_B for $k<2k_F$. The structure function for all interacting fluids is quite similar: it is small for small wave vectors, and rises to unity at about $k=\rho^{1/3}$.

TABLE X. First-order Wu-Feenberg energies and their deviations from variational results for the potential $P5$ (primes denote WF results). E_J is the sum of the potential energy and Jastrow kinetic energy, T_D the Slater kinetic energy, and E the total energy in MeV. S_0 is the structure factor at $k=0$, $\mathcal{E}$ the average Pauli condition.

ρ	E'_J	$E_J-E'_J$	T'_D	$T_D-T'_D$	E'	$E-E'$	S_0	$\mathcal{E}$
0.17	52.4	5.5	33.0	−1.3	85.4	4.2	−0.73	3.05
0.30	119.7	14	46.6	−4.9	166.3	8.6	−0.69	7.37
1.0	657.2	52	100.1	−1.3	757.2	51	−0.63	4.96
2.0	1687	162	158	−31	1845	131	−0.64	8.80
4.0	4346	328	256	−22	4602	306	−0.065	7.74

The second-order term as calculated by Schiff and Verlet[2] appears to be in the wrong direction for zero pressure ^{3}He so the convergence of the whole series for T_D is still questionable. The first-order structure function S' will always be negative, for the same reason that T_D is a good approximation: it only depends on the low k part of S_B.

In addition, Tables IX and X contain the values of the average Pauli condition. It has been suggested[34] that $\mathcal{E}$ defined by

$$\mathcal{E} = \rho \int d^3r (1 - e^{-u(r)}) g_{\mathrm{HF}}(r) \tag{49}$$

might be a convergence parameter for the Brueckner expansion. $\mathcal{E}$ may also be useful as a convergence parameter for the WF expansion. However it is large for these two systems, and its dependance on density is not monotonic for the potential $P5$. For the "Nosanow" system ($P2$) with wave function $W4$, $\mathcal{E}$ is smaller (0.25), but the WF approximation does not appear to be any better. A good convergence test for the WF expansion is more likely the value of the structure factor at small k, since the expansion seems to have the most trouble there. A small error in S_0 can lead to a major error in the energy. It may be also useful to look at the spin-dependent structure factors, since they contain more detailed information.

In conclusion, the WF expansion does not converge quickly for any of the liquids studied in this paper. It is unlikely that inclusion of the next order will substantially increase the precision of the expansion at all densities. Since the magnitude of the errors we have found with the P_5 potential is roughly the same as the difference between our energies and those of Nosanow and of Pandharipande *et al.*, their lower energies can perhaps be ascribed to their use of WF.

Finally, consider the van Kampen permutation[23] expansion in the solid phase. The convergence of this expansion is probably controlled by the localization of the particles on the lattice sites (i.e., C of $W2$). In solid helium changing the product of Gaussians to a determinant of Gaussians made little difference in the energy, since the localization was already high. The zero-order term was enough. However, for the weakly localized crystal of Nosanow[13] the convergence of the expansion was quite poor. We conclude that the use of this expansion may be limited to reasonably-well-localized crystals.

IV. CONCLUSION

We have shown that the Monte Carlo sampling of the square of the antisymmetric wave function is certainly feasible, and probably the only accurate way of getting good upper bounds to the energy of a dense Fermi fluid. The Wu-Feenberg approximation can lead to significant errors in a Lennard-Jones fluid at high densities, and to serious errors for soft-core potentials. We believe that this approximation should be used with great caution in any fermion system. The energy of solid ^{3}He is hardly affected by the Fermi statistics; other physical quantities such as the pressure and Lindeman's ratio seem to be more sensitive. We have determined an approximate phase diagram of fermions interacting with a Yukawa potential. By extrapolating the liquid-solid phase boundary, we have estimated the melting density of the Wigner crystal.

We believe that a realistic calculation of the crystallization density of neutron matter is extremely difficult. First, the Schrödinger equation is not a good description of relativistic neutrons. Second, the crystallization density is highly sensitive to the nucleon-nuoloon interaction. If the "quantumness parameter" of the system is too large, ($\Lambda^* \gtrsim 0.72$) the nucleons will never solidify. For crystallization, the important part of the potential is its form for small r which is not yet well known. Third, various approximations to the ground-state energy can drastically change the solidification density. We believe that the Gaussian wave function is a good approximation to the true crystal ground state, probably much better than the Jastrow function used for the liquid. For this reason, a variational calculation will tend to favor the solid phase. For a soft-core potential, the energies of the liquid and solid phase are very close throughout a large range of densities. In order to obtain a good value for the transition density, one must calculate the ground-state energy very precisely.

Future developments will concern ways to simulate larger systems, improvements in the variational wave function, and the study of different and more complex systems. The presence of nodes in the ground state of a fermion system, precludes the use of the same Monte Carlo algorithm used to find the exact ground state of Bose systems. If one assumes a particular nodal surface for the ground state, for example the nodes of the free Fermi gas, one can find the lowest energy state with those nodes. For most systems this may be a very good approximation to the exact ground state energy. Development of an exact fermion algorithm appropriate to a large ensemble of particles, hinges on an understanding of the nodal surface of the true ground state.

APPENDIX

In this Appendix, we describe two other methods for sampling the square of a determinantal wave

function. Although for the problems we considered, neither of these methods were as good as the one described in the text, there are other systems in which these methods may be effective.

1. Feynman upper bound

The first method uses the Feynmann form for the energy of a product wave function. If ψ_B is an eigenfunction of the Schrödinger equation with an eigenvalue E_B, then the energy of the wave function $\psi_B F$ is given by

$$E_F = E_B + \frac{\hbar^2}{2m} \int dR\, |\psi_B|^2\, |\nabla F|^2 \Big/ \int dR\, |\psi_B F|^2 \,. \tag{A1}$$

Let us choose ψ_B to be the boson ground-state wave function and F an antisymmetric function of spin and spatial coordinates. Then the energy in (A1) will be an upper bound to the fermion ground-state energy. Using the Green's function Monte Carlo method, we can evaluate E_B exactly, and generate configurations (R_i) drawn from the distribution $|\psi_B|^2$. Then for a sufficiently large set of configurations, an upper bound to the fermion energy is estimated from

$$E_F' = E_B + \frac{\hbar^2}{2m} \sum_i |\vec{\nabla} F(R_i)|^2 \Big/ \sum_i |F(R_i)|^2 \,. \tag{A2}$$

Let us choose F to be a Jastrow function ψ_J times D, a Slater determinant of plane waves. Suppose there are g spin states for each spatial state. If g is greater than 1, we must partition the Bose particles into the g spin states; for N particles there are $N!/(I!)^g$ of doing this partition, where $I = N/g$. In order to calculate the most important contributions to the energy integral, one must sample a number of different partitions for each R_i. We tried doing a Metropolis random walk in this partition space, with D^2 as a probability density; D^2 is clearly highly dependent on the partition. For example D^2 is very small if all of the "up" spins are close together. With this method the upper bound is

$$E_F = E_B + \frac{\hbar^2}{2m} \sum_i \left| \frac{\vec{\nabla}_i(\psi_J D)}{D(R)} \right|^2 \Big/ \sum_i \psi_J(R_i)^2 \,. \tag{A3}$$

However, the need to partition complicates the method, and is symptomatic of a fundamental difficulty: unless the function F^2 has its region of maximum probability in the same region of configuration space in which ψ_B^2 is large, configurations drawn from ψ_B^2 will miss the most important region of configuration space for evaluating the energy integrals. Unless F is spatially slowly varying, of the same order of magnitude everywhere, this energy upper bound is likely to be unreliable. But an antisymmetric function can never be slowly varying, since it must have nodes.

This method may be useful in other situations, but only if the weights $F^2(R_i)$ in the denominator of (A2) are of the same order of magnitude, and the probability distributions $|\psi_B|^2$ and $|F\psi_B|^2$ overlap to a significant degree.

2. Multiparticle Metropolis random walk

In the usual Metropolis method for sampling a given ψ^2, only a single particle is moved at a time. Most of the results in the paper were calculated with this method. We have also used a Metropolis method where all of the particles of the same spin are moved simultaneously. Ordinarily this would cause the acceptance ratio of the random walk to become very small, since the chance of moving to an improbable configuration increases with the number of particles.

To compensate for this, the moves were made with a nonuniform probability distribution; we "aimed" the moves toward the region where the wave function was large. For simplicity assume that the particles are all of one spin species ($g = 1$). Let R be the coordinates of the particles, and suppose we choose new trial coordinates R' from the probability function $K(R \to R')$. The new coordinates are accepted with probability

$$P(R \to R') = \min\left(1, \frac{K(R' \to R)\psi^2(R')}{K(R \to R')\psi^2(R)}\right). \tag{A4}$$

It is easy to check that this algorithm satisfies the detailed balance condition:

$$\psi^2(R)K(R \to R')P(R \to R') = \psi^2(R')K(R' \to R)P(R' \to R)\,, \tag{A5}$$

and hence the sequence of steps of the random walk will lead to a density which approaches $\psi^2(R)$ asymptotically.

The acceptance ratio of the random walk can be made close to unity if the transition probability $K(R \to R')$ approximates $\psi^2(R')/\psi^2(R)$. Construct a domain $D(R)$ about each point R. Suppose we could sample the transition function K^* where

$$K^*(R \to R') = \begin{cases} 0, & R' \notin D(R)\,, \\ \psi(R')^2 \Big/ \int_{D(R)} dR''\, \psi^2(R''), & R' \in D(R). \end{cases} \tag{A6}$$

The average acceptance ratio at the point R for this transition function is

$$\int_{D(R)} dR'\,\psi^2(R') \times\left[\max\left(\int_{D(R)} dR''\,\psi^2(R''),\ \times\int_{D(R')}\psi^2(R'')\,dR''\right)\right]^{-1} \tag{A7}$$

Now if D is large enough $\int_{D(R)} dR''\,\psi^2(R'')$ will be roughly independent of R and the acceptance ratio will be almost one. Of course when D becomes the entire space, K^* is simply ψ^2, which we cannot sample. To increase the acceptance ratio of the random walk, we must find a form of $K(R\to R')$ which we can sample and which is an acceptable approximation to K^* in D. Expand the wave function ψ in a Taylor series about the point R, and let D be a Cartesian product of spheres of diameter Δ centered about each particle. Then if the wave function is ψ slowly varying in D, a good approximation to K^* is

$$K_1(R\to R')=\prod_{i=1}^{I}\frac{[1+\vec{G}_i(\vec{r}_i'-\vec{r}_i)]^2}{1+\Delta^2G_i^2/20}\,,$$
$$\vec{G}_i=\vec{\nabla}_i\ln\psi(R)\,. \tag{A8}$$

This probability distribution was sampled by a rejection technique: for each particle (i) a random point x_i uniformly distributed inside a sphere of diameter Δ centered at the origin, is chosen. This point is accepted if

$$(1+\vec{G}_i\cdot\vec{X}_i)^2\geq\xi(1+|G_i|\tfrac{1}{2}\Delta)^2\,, \tag{A9}$$

where ξ is a random number between zero and one. Otherwise the pair $\vec{x}_1$ and ξ is rejected and a new pair is generated and tested to see if they will satisfy condition (A9). The process continues until a satisfactory pair $\vec{x}_1$ and ξ is found. Then the trial position of particle i is $\vec{r}_i'=\vec{r}_i+\vec{x}_i'$. After the new positions have been found for each particle, the probability P [Eq. (A4)] of acceptance of the step R' must be calculated.

$$P=\min\left(1,\ \frac{\psi^2(R')}{\psi^2(R)}\times\prod_{i=1}^{I}\frac{(1+\frac{1}{20}\Delta^2G_i^2)(1-\vec{G}'\cdot\vec{X}_i)^2}{(1+\frac{1}{20}\Delta^2G_i'^2)(1+\vec{G}_i\cdot\vec{X}_i)^2}\right)\,. \tag{A10}$$

For a wave function which is a Slater determinant, evaluating the wave function involves inverting the Slater matrix $D_{ij}(R')$ which will take on the order of I^3 operations, since every element of the matrix changes. Then, for this method to be as effective as the standard Metropolis algorithm, the step sizes Δ should be about the same, since the standard algorithm takes on the order of I^3 operations to move all of the particles.

We have sampled the wave function of liquid ^{3}He using the two different methods ($\rho=0.237/\sigma^3$ and $I=27$). For a step size of 1.3, the one-by-one method had an acceptance ratio of 0.42; for a step size of 0.9 the multiparticle method had an acceptance ratio of 0.15. To get the same error in such quantities as the energy and the structure factor, the multiparticle method took about ten times longer. Thus this multiparticle method converged significantly more slowly than the method of moving one particle at a time. For more particles the situation would be even worse. Hence, we believe that for the types of wave functions considered in this paper the standard Metropolis method, where particles are moved one at a time, is superior to the multiparticle method.

We have tried two other variants for the transition function $K(R\to R')$. The first is to let the domain $D(R)$ be a product of cubes centered about R and of side D. The other is to allow second-order terms into K

$$K_2(R\to R')=\prod_{i=1}^{I}\frac{[1+G(r_i'-r_i)+T(r_i'-r_i)^2]^2}{1+\frac{1}{20}\Delta^2G^2+\frac{6}{5}\Delta^2T+\frac{3}{7}\Delta^4T^2}\,,$$
$$T=\langle\nabla^2\psi/\psi\rangle\,. \tag{A11}$$

Neither change affected the random walk in a significant way.

However, there may be problems for which the multiparticle method is applicable. If one has a wave function with just a few particles in a spin state, it may be convenient to move them together. Inverting a matrix all at once is about twice as fast computationally as inverting it one row at a time. If the particles of like spin are well separated from each other the linear approximation for K will be good. Finally, the multiparticle method would appear to be well suited for determinantal wave functions where each matrix element depends on the coordinates of each particle. An example is the backflow wave function, due to Feymann, for a Fermi liquid such as ^{3}He. The orbitals in this wave function are

$$\rho_{k_i}(r_i)=\exp\left[ik_i\cdot\left(\vec{r}_i+\sum_{j}^{N}(\vec{r}_i-\vec{r}_j)g(r_{ij})\right)\right]. \tag{A12}$$

If a single particle is moved all of the matrix elements are changed, and so the entire matrix must be reinverted. Hence in the standard Metropolis algorithm this would take I^4 operations to move all of the particles. However the multiparticle method takes only I^3 operations. The implied ratio of computing times is valid only if the step sizes and acceptance ratios are approximately equal.

†Supported by the ERDA under Contract No. EY-76-C-02-3077*000 and by Grant No. DMR-74-23494 with the NSF and in part by the NSF through the Materials Science Center, Cornell University, under Grant No. DMR-72-03029.

[1]W. L. McMillan, Phys. Rev. 138, A442 (1965).
[2]L. Schiff and L. Verlet, Phys. Rev. 160, 208 (1967).
[3]M. H. Kalos, D. Levesque, and L. Verlet, Phys. Rev. A 9, 2178 (1974).
[4]D. M. Ceperley, G. V. Chester, and M. H. Kalos (unpublished).
[5]M. H. Kalos, Phys. Rev. A 2, 250 (1970).
[6]B. H. Brandow, Phys. Lett. B 61, 117 (1976).
[7]N. Metropolis, A. W. Rosenbluth, M. N. Rosenbluth, A. H. Teller, and E. Teller, J. Chem. Phys. 21, 1087 (1953).
[8]H. W. Jackson and E. Feenberg, Ann. Phys. (N.Y.) 15, 266 (1961).
[9]R. P. Feynman, Phys. Rev. 94, 262 (1954).
[10]The averages in Eq. (20) are done with configuration drawn from $|\psi_J D|^2$. However, if ψ_J is an eigenfunction of H, then E_j is its eigenvalue.
[11]S. G. Cochran, thesis (Cornell University, 1973) (unpublished).
[12]For a *homogeneous* system $n(r) = \langle \psi(r_1+r)/\psi(r_1) \rangle$. But $n^2(r) \leq \langle (\psi(r_1+r)/\psi(r_1))^2 \rangle = 1$.
[13]L. H. Nosanow and L. J. Parish, Ann. N. Y. Acad. Sci. 224, 226 (1973).
[14]Our calculations were done on the CDC 6600 computer at the Courant Institute, New York University. For the largest system we simulated, 128 particles, moving all of the particles once took 5 sec (acceptance ratio: 0.4) with this computer we could have simulated up to 300 particles in a reasonable amount of time.
[15]The maximum observed error in Eq. (10) was 10^{-10}.
[16]C. M. Care and N. H. March, Adv. Phys. 24, 101 (1975).
[17]F. Y. Wu and E. Feenberg, Phys. Rev. 128, 943 (1962).
[18]The Fourier transform of $n(r)$ is not accurate, because the system is so small, $n(\vec{r})$ for 114 particles is not spherically symmetric, and Fourier transforming and sphericalizing do not commute.
[19]V. R. Pandharipande and H. A. Bethe, Phys. Rev. C 7, 1312 (1973).
[20]J. P. Hansen and D. Levesque, Phys. Rev. 165, 293 (1968).
[21]Our results imply that v solid is $\sim 26 \pm 1$ cm^3/mole and v liquid is $\approx 30 \pm 1$ cm^3/mole; the experimental values are 24.5 and 25.8, respectively.
[22]G. Baym and C. J. Pethick, Ann. Rev. Nucl. Sci. (1975).
[23]N. G. van Kampen, Physica (Utr.) 27, 783 (1961); L. H. Nosanow, Phys. Rev. 146, 120 (1966).
[24]We define Lindemann's ratio as the root-mean square distance to the *nearest* lattice site divided by the nearest-neighbor distance. The liquid value is an upper limit to this number.
[25]V. R. Pandharipande, R. B. Wiringa, and B. D. Day, Phys. Lett. B 57, 205 (1975).
[26]V. R. Pandharipande, Nucl. Phys. A 248, 524 (1975).
[27]S. Chakrauarti *et al.*, Nucl. Phys. A 220, 233 (1974); V. Canuto and S. M. Chitre, Phys. Rev. D 9, 1587 (1974); L. Shen and C. Woo, *ibid.* 10, 371 (1974); M. T. Takemori and R. A. Guyer, *ibid.* 11, 2696 (1975).
[28]This potential with $\Lambda^* = 0.93$ was first suggested as a model potential for a simple model of neutron matter. It was proposed by H. A. Bethe as a "homework" problem to the people working in the field of neutron matter, and has become known as the "homework" potential.
[29]S. G. Brush, H. L. Sahlin, and E. Teller, J. Chem. Phys. 45, 2102 (1966).
[30]F. Y. Wu, H. T. Tan, and E. Feenberg, J. Math. Phys. 8, 864 (1967).
[31]The Gaussian model is a wave function equal to a product of Gaussians centered at the lattice sites; the sum of the potential and kinetic energies is minimized with respect to the localization of the Gaussians.
[32]H. R. Glyde, G. H. Keech, R. Mazighi and J. P. Hansen, Phys. Lett. A 58, 226 (1976).
[33]R. Monnier, Phys. Rev. A 6, 393 (1972); C. W. Woo, Phys. Rev. 151, 138 (1966).
[34]J. W. Clark and M. L. Ristig, Phys. Rev. C 5, 1553 (1972).